Identification and magneto-optical properties of the NV center in 4*H*-SiC

H. J. von Bardeleben,[1,*] J. L. Cantin,[1] E. Rauls,[2] and U. Gerstmann[2]

[1]*INSP, Université Pierre et Marie Curie, UMR 7588 au CNRS 4 place Jussieu, 75005 Paris, France*

[2]*Lehrstuhl für Theoretische Physik, Universität Paderborn, Warburger Strasse 100, 33098 Paderborn, Germany*

(Received 13 February 2015; revised manuscript received 13 July 2015; published 6 August 2015)

Single spin carrying defects are key elements in quantum information and nanosensing technology with the nitrogen-vacancy (NV) center in diamond being the outstanding example. In a combined electron paramagnetic resonance and first-principles modeling study we verify the existence of such NV centers in 4*H*-SiC in the form of silicon vacancy-nitrogen pairs ($V_{Si}N_C$) and explore their basic magneto-optical properties. Similar to the NV center in diamond, the $^3A_2$ triplet ground state (with a zero-field splitting of $D = 429 \times 10^{-4}$ cm^{-1}) of the singly negative charge state in axial coordination can be optically spin polarized at room temperature. Given the mature technology of 4*H*-SiC the NV center in this material is expected to play an important role in future spintronics applications.

DOI: 10.1103/PhysRevB.92.064104 PACS number(s): 76.30.−v, 61.72.jd, 71.55.−i

I. INTRODUCTION

Spin carrying defects in solids, the state of which can be optically written and read, have recently become attractive systems for their application as qubits [1–5]. It has been shown in recent years that the nitrogen-vacancy (NV) center in diamond is a system with outstanding properties [6,7]. The name NV center is the acronym for the nitrogen donor carbon-vacancy close pair defect. In the negative charge state it provides spin triplets, i.e., a $^3A_2$ ground and a ^3E excited state with zero-field splittings of 2.88 and 1.42 GHz, respectively. Due to weak coupling to the lattice, zero-phonon radiative transitions can be observed even at room temperature. As a nonradiative recombination path via an intermediate singlet state is operating in parallel, the spin ground state can be optically prepared in the $m_s = 0$ state, and the result can be optically read out. The NV center in bulk and nanocrystalline diamond has, thus, given rise to numerous applications in the fields of quantum information and nanoscale metrology. Their magnetic and optical properties are sensitive to magnetic fields, electrical fields, temperature, and strain, thus nanocrystals containing single NV centers allow their measurement with nanometric resolution [8,9].

The results obtained for the NV center in diamond have stimulated the search for similar defects in alternative materials with superior material properties [2–5]. Recently, silicon carbide has been proposed as such a material [10–16], whereby Si vacancies (V_{Si}^-) [14–18], divacancies ($V_{Si}V_C$) [10,19–21], and carbon antisite-vacancy pairs ($C_{Si}V_C$) [13] serve as controllable spin states with sharp zero-phonon lines (ZPLs). Based on theoretical studies, also the direct equivalent of the NV center in diamond, a negatively charged ($V_{Si}N_C$) center in 4*H*-SiC with V_{Si} and N_C on adjacent lattice sites, has been proposed as a defect with outstanding properties similar to those of the NV prototype in diamond [2]. The NV center in SiC is expected to have an exceptionally high impact as silicon carbide is a technologically important and well-understood semiconductor compound in which critical issues, such as point defect formation, *n*- and *p*-type doping, as well as nanostructuring are fully mastered. It is, thus, of high interest to verify the existence of such NV centers in SiC and explore their basic magneto-optical properties. Theoretical predictions have shown that NV centers should be stable in SiC, independent of the polytype [22,23]. The desired spin triplet of the negative charge state is predicted to be stable for Fermi levels in a 1-eV broad range below the conduction band. The zero-phonon line of the absorption between the $^3A_2$ ground state and the ^3E excited state is expected slightly below 1.1 eV, similar to that of the divacancy in SiC and much smaller than the one in diamond (1.95 eV).

We present here the results of a combined electron paramagnetic resonance (EPR) and theoretical study in which we investigate this NV center in 4*H*-SiC. Thereby, our paper is organized as follows: After a description of the experimental and theoretical methods, the identification of the NV center is illustrated and explained in detail in Sec. IV A. Finally, we show in Secs. IV B and IV C that optical polarization of the ground state is indeed very similar to that of the NV center in diamond, whereby in 4*H*-SiC: (i) the sensitivity with temperature is found to be two times larger, and (ii) the PL spectrum is indeed shifted towards the near infrared.

II. EXPERIMENTAL DETAILS

The samples used in this study were commercially purchased N-doped (2×10^{17}-cm^{-3}) *n*-type 4*H*-SiC bulk samples. The free-standing 300-μm-thick samples have been irradiated at room temperature with 12-MeV protons to fluencies up to 10^{16} cm^{-2}. At this energy the protons cross the sample to fully extend. Due to elastic collisions they will generate atomic displacements and, thus, introduce predominantly vacancies and interstitials in the two sublattices. The main paramagnetic point defects observed after this irradiation are silicon and carbon monovacancies V_{Si}, V_C and carbon dumbbells $(C\text{-}C)_C$. To generate NV centers the samples were then subsequently annealed at 900 °C. The EPR measurements were performed with commercial Bruker spectrometers in the 9-GHz (*X* band) and 35-GHz range (*Q* band) under standard conditions in the 4–300-K temperature range, whereby an exact orientation of the samples with respect to the external magnetic field is controlled by laser interferometry. The magneto-optical

*vonbarde@insp.jussieu.fr

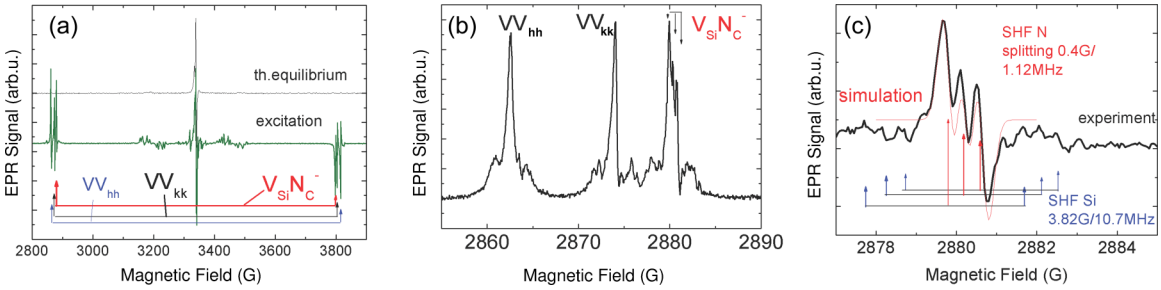

FIG. 1. (Color online) Optically induced EPR spectra of the $V_{Si}N_C^-$ and divacancy centers in 4H-SiC: (a) X-band EPR spectrum at $T = 4$ K and $B \parallel c$ before (top) and after photoexcitation (bottom) displaying three spin $S = 1$ centers with splitting of around 900 G; (b) higher-resolution spectrum and (c) very high-resolution spectrum of the low-field line showing the resolved triplet structure of the NV center.

properties were studied by photo-EPR using different light sources (high-pressure mercury lamp, tungsten halogen lamp, and lasers) emitting in the visible and near-infrared spectral range.

After irradiation and annealing the samples show under thermal equilibrium conditions different spin $S = 1/2$ defects close to a g value of 2.0028, which will not be discussed here. Further three spin $S = 1$ centers with zero-field splittings around 440×10^{-4} cm^{-1} are observed [cf. Figs. 1(a)–1(c)]. From previous studies [19,20] two of them can be identified as neutral axial divacancies ($V_{Si}V_C$ centers) on nearest-neighbor hexagonal (hh) and quasicubic (kk) lattice sites, respectively. The additional axial spin $S = 1$ center, is the central object of this study. With 429×10^{-4} cm^{-1} it shows a zero-field splitting slightly smaller than that of the axial divacancies, but different from the divacancy centers it has a particular triplet structure with equal intensity and equidistant splitting [cf. Figs. 1(b) and 1(c) for the low-field lines]. The triplet splitting can be followed under angular variation in the external magnetic field, which excludes a superposition of defects, e.g., basal, 71° off-axis-oriented divacancies as an origin. Instead, it is the clear fingerprint of an isotropic hyperfine (HF) interaction with a close to 100% abundant nuclear spin $I = 1$ and identifies the HF interaction as due to a single ^{14}N nitrogen nucleus. The HF splitting is small—0.38 G (1.12 MHz)—but well resolved due to an EPR linewidth below 0.3 G. The NV center shows additional superhyperfine (SHF) interaction with Si neighbors, which is best resolved at $T = 100$ K [cf. Fig. 1(c)]. It corresponds to a SHF splitting of 3.82 G (10.7 MHz) and an interaction with *three* equivalent Si neighbors. The spin Hamiltonian parameters, which are the basis for the identification of the defect, have been deduced from the angular variation in the EPR spectra [Fig. 2(a)] using the following spin Hamiltonian:

$$H = \mu_B S g B + S D S + \sum_k S A_k I_k,$$

where the symbols have the usual meaning: μ_B is the Bohr magneton, S is the electron spin, g is a tensor, B is the applied magnetic field, D is a zero-field splitting tensor, A_k is a hyperfine tensor, and I_k is the nuclear spin of the corresponding nuclei k. The parameters D and g at $T = 4.2$ K were obtained by fitting the observed angular variation in the EPR line resonance fields. Besides the hyperfine splittings already given above, within axial C_{3v} symmetry, we obtain the following values: $D = 3/2D_{zz} = +429 \times 10^{-4}$ cm^{-1} (1286 MHz), $E = 1/2(D_{xx} - D_{yy}) = 0$, and $g_{iso} = 2.003 \pm 0.001$.

In Fig. 2(b) we show the energy levels of the $^3A_2$ ground state for $B \parallel c$ and the associated EPR transitions. In the Q band, the new $S = 1$ center can be already observed at thermal equilibrium conditions [cf. Fig. 2(c)] and is, thus, a ground-state configuration. Under photoexcitation, however, its intensity is increased, and the low-field and high-field lines are observed with different phases, i.e., in absorption and emission, respectively, indicating an optically induced preferential population of the $m_s = 0$ state [cf. Fig. 2(d)].

III. COMPUTATIONAL METHOD

To identify this defect we performed comparative first-principles calculations in the framework of density functional theory (DFT). For the theoretical modeling of the defect states

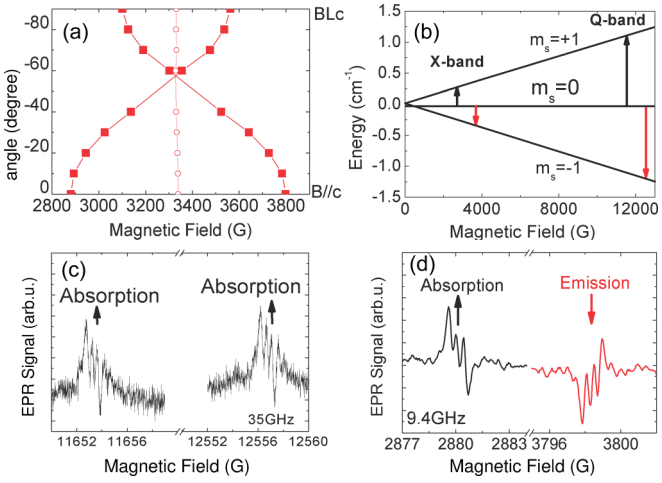

FIG. 2. (Color online) (a) Angular variation in the $V_{Si}N_C^-$ EPR spectrum for a rotation of the magnetic field in the $(11\bar{2}0)$ plane; the nonisotropic center of gravity of the two lines is also indicated. (b) Energy levels of the $^3A_2$ ground state showing a level crossing at 500 G and the X-band and Q-band EPR transitions under optical polarization; absorption (black), emission (red). (c) Q-band EPR spectrum taken at $T = 295$ K under thermal equilibrium conditions; both lines are in absorption. (d) X-band EPR spectrum at $T = 4$ K under optical excitation with 2.4 eV showing the optically induced polarization of the ground state: The low-field line is observed in absorption, and the high-field line is observed in emission.

we use supercells containing up to 432 atoms, standard norm-conserving pseudopotentials, and a plane-wave basis with an energy cutoff of 50 Ry. All defect structures have been fully relaxed using equidistant $2 \times 2 \times 2$ Monkhorst Pack k-point samplings and the spin-polarized Perdew-Burke-Ernzerhof (PBE) functional [24]. For the calculation of transition energies the Heyd-Scuseria-Ernzerhof (HSE) hybrid functional [25] has been used. The EPR parameters are calculated taking into account relativistic effects: Whereas the HF splittings are determined in scalar relativistic approximation by the magnetization density $m(r)$ in a very small region around the nuclei [26], the deviations of the g tensor from the free-electron value 2.002 319 are driven by spin-orbit coupling as mediated by the spin currents $j(r)$ induced by the external magnetic field [27,28]. To calculate these characteristic g-value shifts, we use the gauge-including projector augmented plane-wave approach [28] as implemented in the QUANTUM-ESPRESSO package [29].

IV. RESULTS AND DISCUSSION

A. EPR signatures

We calculate the magnetic signature of the spin $S = 1$ triplet states of axial $V_{Si}N_C$ pairs as well as for the corresponding divacancy defects (Table I). The comparison of the DFT data with the experimentally determined spin Hamiltonian parameters, namely, the symmetry, electron spin S, g factor, HF interactions $A(^{14}N)$, $A(^{29}Si)$ allow us to identify the microscopic structure of the new $S = 1$ center as the negatively charged $V_{Si}N_C^-$ defect, i.e., the NV center [31]. In particular, the resolved ^{14}N HF splitting makes this identification unambiguous. Although we cannot distinguish experimentally between the (hh) and the (kk) $V_{Si}N_C^-$ pairs—the difference in the g-tensor values is too small to be resolved (cf. Table I)–-the appearance of a triplet splitting proves that N atoms are involved and, thus, excludes purely intrinsic defects, such as divacancies as a model. Thereby, the perfect agreement of the measured values extracted from the fit of the spectra and the average value predicted by theoretical modeling (both 1.12 MHz) might appear fortuitous. However, due to the HF interaction of the minority spin dominating the region around the ^{14}N nucleus, it is quite robust against technical details of the calculation, e.g., the choice of the XC functional. Actually, for a local density approximation functional (Perdew-Zunger) [32] and the HSE hybrid functional [25], we obtain values of -0.85 and -1.29 GHz, respectively, quite similar to the PBE values shown in Table I. The observed zero-field splitting is close to that of the one predicted for the axial divacancies in 4H-SiC [30], a result further in support of our assignment. Very recently a different spin $S = 1$ center with much larger zero-field splitting has been tentatively attributed to an NV center in 6H-SiC [33]. In view of the present results this assignment should be reconsidered.

The similarity of the g values and zero-field splitting of the NV center and the divacancies (Table I) might at first be surprising; but as can be seen in Figs. 3(a) and 3(b) the magnetization density is mainly localized at the carbon

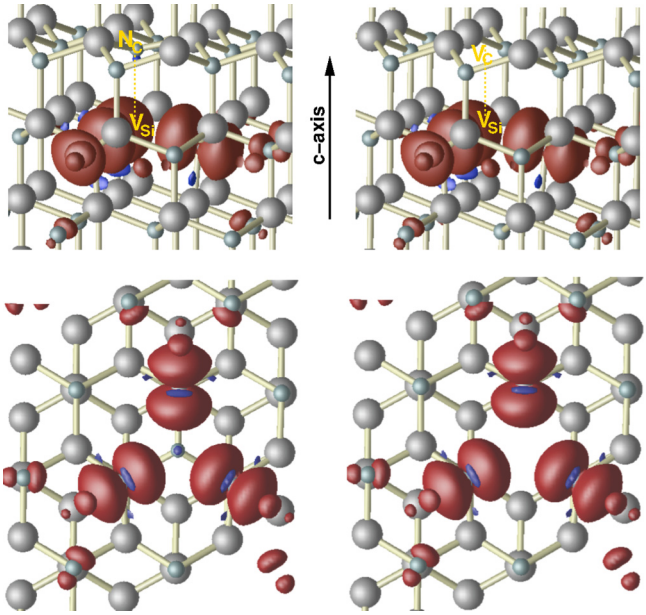

FIG. 3. (Color online) Calculated spin-density distribution (*top*: side view; *bottom*: view along the hexagonal c axis) for the axial (hh) triplet centers in 4H-SiC, both dominated by the (V_{Si}-C_3) core structure: For the $V_{Si}N_C^-$ center (*left*) only a very small part of the minority spin (negative sign of a_{iso} in Table I) is found at the ^{14}N nucleus, missing in the divacancy center (*right*).

TABLE I. Experimental and calculated values of the g tensor and hyperfine parameters (MHz) for the axial $V_{Si}N_C^-$ centers and divacancies; experimental values for the D parameter are also given. Experimentally, the two axial configurations (hh and kk) cannot be distinguished as the differences in all the EPR parameters are below the resolution. Calculated transition energies (HSE hybride functional for a 192 atom supercell) for the ($^3A_2$-^3E) ZPL are in the case of the divacancy identical with a value of 1.05 eV from Ref. [30], close to the experimental value of 1.09 eV [10].

Model	ZPL (eV)	g_{xx}	g_{yy}	g_{zz}	D_{exp} (10^{-4}/cm)	($1 \times ^{14}N$) a_{iso}	($3 \times ^{29}Si$) a_{iso}	($3 \times ^{13}C$) A_{xx}, A_{yy}, A_{zz}
$V_{Si}N_C^-$, expt.	0.95[a]		$g_{iso} = 2.003$		+429	±1.12	10.7	
$V_{Si}N_C^-$, hh	0.99	2.00293	2.00293	2.00353	+429	−1.09	10.3	63.2, 62.4, 133.3
$V_{Si}N_C^-$, kk	0.97	2.00293	2.00293	2.00362	+429	−1.15	11.0	56.4, 55.6, 126.2
$V_{Si}V_C$, hh	1.05	2.00235	2.00235	2.00372	+445		10.0	65.8, 65.0, 134.9
$V_{Si}V_C$, kk	1.05	2.00255	2.00255	2.00365	+434		10.5	60.4, 59.7, 129.2

[a]For $V_{Si}N_C^-$ the experimental value is determined via the center of the multiphonon line; the corresponding ZPL should be slightly larger.

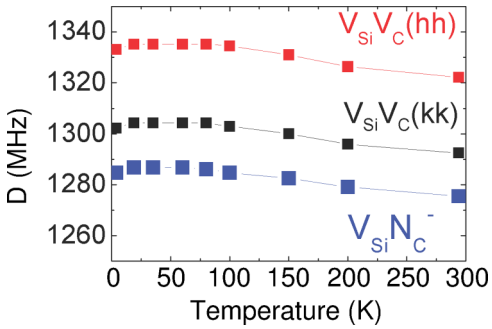

FIG. 4. (Color online) Variation with temperature in the zero-field splitting parameter of the $V_{Si}N_C^-$ center (and its fit with a third-order polynomial) compared with the values of the axial divacancies $V_{Si}V_C$ (hh,kk).

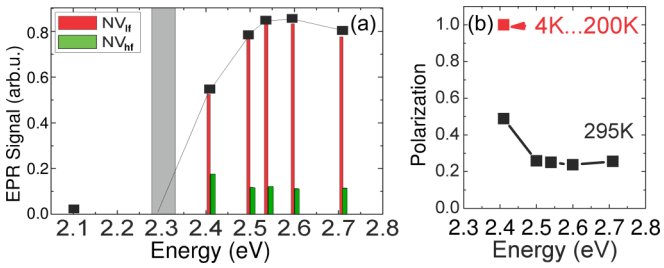

FIG. 5. (Color online) Optically induced spin polarization of the $V_{Si}N_C^-$ center [Ar-ion laser and one diode laser (2.1 eV) with 100-mW excitation]: (a) Photoexcitation spectrum at $T = 295$ K showing a threshold at 2.3 eV; the ground-state populations for the low-field (red bar) and high-field lines (green bar) are also shown. (b) Temperature dependence of the ground-state polarization; below 200 K only the $m_s = 0$ state is populated, and at 295 K we have a fractional occupation of the $m_s = +1$ state.

dangling bonds of the V_{Si} component of the defect pair. Only a very small part of the density of the unpaired electrons is found at the nitrogen ^{14}N nucleus. Accordingly, the magnetization density giving rise to the HF splitting as well as the spin-spin part of the zero-field splitting resembles nearly perfectly that of the divacancy. For both kinds of defect, the electronic properties are mainly determined by the (V_{Si}-C_3) core structure of the defect. Consequently, the $V_{Si}N_C^-$ pairs provide HF splittings with nearest-neighbor C and next-nearest-neighbor Si atoms similar to that of the corresponding divacancies as well as within 3% of the same zero-field splitting parameter D (cf. Table I).

B. Temperature dependence of the fine structure

We have further measured the temperature variation of the zero-field splitting for the NV center as well the axial divacancy centers in the range from 4 to 300 K (cf. Fig. 4). The sensitivity of the D parameter with temperature has been shown to be important for the application of the diamond NV center in nanoscale thermometry [34]. The temperature variation for the triplet centers in 4H-SiC can be fitted with a third-order polynomial. At temperatures below 20 K, the D values slightly increase by 2 MHz from the 4-K values given in Table I to those given in Ref. [20]. Above $T = 70$ K, we observe a monotonous decrease in D, qualitatively quite similar to the case of NV in diamond. In the range of 50–300 K, however, the D-value variation for the NV center in 4H-SiC is with 15 MHz two times higher than the one in diamond where a decrease of 7 MHz over this temperature range has been observed [34]. Following the arguments in Ref. [34] we explain the increased temperature sensitivity in SiC by larger lattice expansion and stronger electron-phonon interactions.

C. Optical pumping and spin polarization

The strong similarities in the electronic structure of the $V_{Si}N_C^-$ center and the divacancies [35,36] suggest similar magneto-optical properties, which in the case of divacancies have been already shown to be promising for quantum spintronics application [10]. Hence, we have investigated the optical pumping of the ground state of the NV center in 4H-SiC (see Fig. 5 and Table I). Similar to the divacancy in this material [10,30], an $^3A_2 \rightarrow {}^3E$ excitation can be obtained directly via the ZPL, higher intracenter transitions, or hole/defect assisted, a frequent phenomenon in SiC. Using the HSE hybrid functional, we calculate an average value of 0.98 eV for the ZPL, i.e., about 0.1 eV less than for the divacancy-related transitions (cf. Table I). In addition, a lower-energy limit of 2.1 eV for a hole-assisted excitation is predicted. And indeed, we were able to detect the NV center related room-temperature PL, which is centered at 0.95 eV (1.3 μm), i.e., about 0.1 eV lower in energy than usually observed for divacancy-related PL spectra in 4H-SiC (see, e.g., Ref. [10]). Above 2.3-eV excitation we do also observe a broad absorption range with slightly varying properties [cf. Fig. 5(a)], which can be efficiently used for optical polarization of the ground state: Similar to the case of NV centers in diamond the optical excitation induces a strong spin polarization of the $^3A_2$ ground state with a predominant population of the $m_s = 0$ state [cf. Fig. 2(b)] providing a control of the spin state facilitating qubit manipulation. The polarization can be read out by EPR via the amplitudes and phases of the low- and high-field resonance lines corresponding to the magnetic dipole allowed $m_s = \pm 1 \rightarrow m_s = 0$ transitions: In thermal equilibrium the two lines show equal phases and intensities [cf. Fig. 2(c)]. If a nonthermal equilibrium occupation of the three m_s states is achieved, the corresponding EPR lines are no longer observed with this normal intensity ratio and phase [cf. Fig. 2(d)]. Below $T = 200$ K the ground-state polarization induced by a 2.4-eV photoexcitation is complete: We observe the low-field and high-field EPR lines, respectively, in absorption and emission with equal amplitudes [cf. Fig. 5(b)]. At higher temperatures the high-field line in emission decreases in intensity, changes phase, and is about 20% in intensity relative to the low-field line indicating an increased relaxation from the $m_s = 0$ states to the $m_s = +1$ lower spin state.

V. CONCLUSIONS

To summarize, by EPR spectroscopy we have verified the existence of the negatively charged NV center in 4H-SiC. In agreement with theoretical predictions it displays magnetic and optical properties which make it an extremely promising system for qubit and nanosensing applications: Similar to the

NV prototype in diamond, the singly negative charge state in axial coordination can be optically spin polarized at room temperature, whereby the resulting PL spectrum is shifted to the near infrared. Interestingly, the sensitivity with temperature is found to be twice as large as in diamond. The high level technology of SiC microelectronics proposes an easy extension from bulk samples to sophisticated nanopatterning of low fluence irradiated layers and electrical/magnetic connections to control and measure the spins states of individual and small ensembles of NV centers. The extension to the use of $4H$-SiC nanoparticles with single NV centers for nanomagnetometry and single-photon emitters seems to be straightforward; single-photon emission based on the $C_{Si}V_C$ defect has already been achieved for $3C$-SiC nanoparticles [37].

ACKNOWLEDGMENTS

Numerical calculations were performed using grants of computer time from the Paderborn Center for Parallel Computing (PC^2) and the HLRS Stuttgart. The Deutsche Forschungsgemeinschaft (DFG) is acknowledged for financial support. We thank F. Treussart (ENS, Cachan) for fruitful discussions on the NV center in diamond and M.F. Barthe (CNRS, Orléans) for the proton irradiations.

[1] R. Hanson and D. D. Awschalom, Coherent manipulation of single spins in semiconductors, Nature (London) **453**, 1043 (2009).

[2] J. R. Weber, W. F. Koehl, J. B. Varley, A. Janotti, B. B. Buckley, C. G. van de Walle, and D. D. Awschalom, Quantum computing with defects, Proc. Natl. Acad. Sci. USA **107**, 8513 (2010).

[3] D. DiVincenzo, Better than excellent, Nature Mater. **9**, 468 (2010).

[4] A. Dzurak, Quantum computing: Diamond and silicon converge, Nature (London) **479**, 47 (2011).

[5] A. Boretti, Optical materials: Silicon carbide's quantum aspects, Nat. Photonics **8**, 88 (2014).

[6] F. Jelezko and J. Wachtrup, Single defect centers in diamond: A review, Phys. Status Solidi A **203**, 3207 (2006).

[7] M. W. Doherty, N. B. Manson, P. Delaney, F. Jelezko, J. Wrachtrup, and L. C. L. Hollenberg, The nitrogen vacancy color center in diamond, Phys. Rep. **528**, 1 (2013).

[8] T. Plakhotnik, M. W. Doherty, J. H. Cole, R. Chapman, and N. B. Manson, All-optical thermometry and thermal properties of the optically detected spin resonances of the NV- center in nanodiamond, Nano Lett. **14**, 4989 (2014).

[9] T. P. Tetienne, T. Hignant, J. V. Kim, L. Herrera Diez, J. P. Adam, K. Garcia, J. F. Roch, S. Rohart, A. Thiaville, D. Ravelosona, and V. Jacques, Nanoscale imaging and control of domain wall hopping with a nitrogen-vacancy center microscope, Science **344**, 1366 (2014).

[10] W. F. Koehl, B. B. Buckley, F. J. Heremans, G. Calusine, and D. D. Awschalom, Room temperature coherent control of defect spin qubits in silicon carbide, Nature (London) **479**, 84 (2011).

[11] A. L. Falk, B. B. Buckley, G. Calusine, W. V. V. Dobrovitski, A. Politi, C. A. Zorman, P. X. L. Feng, and D. D. Awschalom, Polytype control of spin qubits in silicon carbide, Nat. Commun. **4**, 1819 (2013).

[12] D. D. Awschalom, L. C. Bassett, A. S. Dzurak, E. L. Hu, and J. R. Petta, Quantum Spintronics: Engineering and manipulating atom like spins in semiconductors, Science **339**, 1174 (2013).

[13] S. Castelletto, B. C. Johnson, V. Ivády, N. Stavrias, T. Umeda, A. Gali, and T. Ohshima, A silicon carbide room-temperature single photon source, Nature Mater. **13**, 151 (2014).

[14] P. G. Baranov, A. P. Bundakova, A. A. Soltamova, S. B. Orlinskii, I. V. Borovykh, R. Zondervan, R. Verberk, and J. Schmidt, Silicon vacancy in SiC as a promising quantum system for single defect and single photon spectroscopy, Phys. Rev. B **83**, 125203 (2011).

[15] D. Riedel, F. Fuchs, H. Kraus, S. Vaeth, A. Sperlich, V. Dyakonov, A. A. Soltamova, P. G. Baranov, V. A. Ilyin, and G. A. Astakov, Resonant adressing and manipulation of silicon vacancy qubits in silicon carbide, Phys. Rev. Lett. **109**, 226402 (2012).

[16] M. Widmann, S. Y. Lee, T. Rendler, N. T. Son, H. Fedder, S. Paik, L.-P. Yang, N. Zhao, S. Yang, I. Booker, A. Denisenko, M. Jamali, S. A. Momenzadeh, I. Gerhardt, T. Ohshima, A. Gali, E. Janzén, and J. Wrachtrup, Coherent control of single spins in silicon carbide at room temperature, Nature Mater. **1**, 4145 (2014).

[17] E. Sörman, N. T. Son, W. M. Chen, O. Kordina, C. Hallin, and E. Janzén, Silicon vacancy related defect in 4H and 6H SiC, Phys. Rev. B **61**, 2613 (2000).

[18] N. Mizuochi, S. Yamasaki, H. Takizawa, N. Morishita, T. Ohshima, H. Itoh, and J. Isoya, EPR studies of the isolated negatively charged silicon vacancies in n-type 4H- and 6H-SiC: Identification of C_{3v} symmetry and silicon sites, Phys. Rev. B **66**, 235202 (2002).

[19] V. S. Vainer and V. A. IIin, Electron spin resonance of exchange coupled vacancy pairs in heaxagonal silicon carbide, Sov. Phys. Solid State **23**, 2126 (1981).

[20] N. T. Son, P. Carlson, J. ul Hassan, E. Janzén, T. Umeda, J. Isoya, A. Gali, and M. Bockstedte, Divacancy in 4H-SiC, Phys. Rev. Lett. **96**, 055501 (2006).

[21] O. V. Zwier, D. O'Shea, A. R. Onur, and C. H. van der Wal, All-optical coherent population trapping with defect spin ensembles in silicon carbide, Sci. Rep. **5**, 10931 (2015).

[22] U. Gerstmann, E. Rauls, T. Frauenheim, and H. Overhof, Formation and annealing of nitrogen complexes in 3C-SiC, Phys. Rev. B **67**, 205202 (2003).

[23] J. R. Weber, W. F. Koehl, J. B. Varley, A. Janotti, B. B. Buckley, C. G. Van de Walle, and D. D. Awschalom, Defects in SiC for quantum computing, J. Appl. Phys. **109**, 102417 (2011).

[24] J. P. Perdew, K. Burke, and M. Ernzerhof, Generalized gradient approximation made simple, Phys. Rev. Lett. **78**, 1396 (1997).

[25] J. Heyd and G. E. Scuseria, Efficient hybrid density functional calculations in solids: Assessment of the Heyd-Scuseria-Ernzerhof screened Coulomb hybrid functional, J. Chem. Phys. **121**, 1187 (2004).

[26] P. E. Blöchl, First principle calculations of defects in oxygen deficient silica exposed to hydrogen, Phys. Rev. B **62**, 6158 (2000).

[27] U. Gerstmann, M. Rohrmüller, F. Mauri, and W. G. Schmidt, *Ab initio* tensor calculations for paramagnetic surface states: Hydrogen absorption at Si surfaces, Phys. Status Solidi C **7**, 157 (2010).

[28] C. J. Pickard and F. Mauri, First principle theory of the EPR g-tensor in solids; defects in quartz, Phys. Rev. Lett. **88**, 086403 (2002).

[29] P. Giannozzi *et al.*, Quantum Espresso: A modular and open source software project for quantum simulations of materials, J. Phys.: Condens. Matter **21**, 395502 (2009), http://www.quantum-espresso.org.

[30] K. Szasz, V. Ivady, E. Janzén, and A. Gali, First principles investigation of divacancy in SiC. polytypes for solid state qubit application, Mater. Sci. Forum **778-780**, 499 (2014).

[31] Note that the stoichiometric equivalent alternative $V_C N_{Si}$ is unstable and relaxes barrier free into the configuration with N residing in the carbon sublattice, cf. Ref. [21].

[32] J. P. Perdew and A. Zunger, Self-interaction correction to density-functional approximations for many-electron systems, Phys. Rev. B **23**, 5048 (1981).

[33] N. Bagraev, D. Gets, E. Kalabukhova, L. Klyachkin, A. Malyarenko, D. Savchenko, and B. Shanina, Electrically detected electron paramagnetic resonance of point centers in 6H-SiC. nanostructures, Semiconductors **48**, 1467 (2014).

[34] M. W. Doherty, V. M. Acosta, A. Jarmola, M. S. J. Barson, N. B. Manson, D. Budker, and L. C. L. Hollenberg, Temperature shifts of the resonances of the NV- center in diamond, Phys. Rev. B **90**, 041201(R) (2014).

[35] A. Gali, A. Gällström, N. T. Son, and E. Janzén, Theory of neutral divacancy in SiC: A defect for spintronics, Mater. Sci. Forum **645-648**, 395 (2010).

[36] F. Pan, M. Zhao, and L. Mei, First-principles prediction of the negatively-charged nitrogen-silicon-vacancy center in cubic silicon carbide, J. Appl. Phys. **108**, 043917 (2010).

[37] S. Castelletto, B. C. Johnson, C. Zachreson, D. Beke, I. Balogh, T. Ohshima, I. Aharonovich, and A. Gali, Room temperature quantum emission from cubic silicon carbide nanoparticles, ACS Nano **8**, 7938 (2014).